FLOW VISUALIZATION OF THE INTERACTION BETWEEN A SOOTBLOWER JET AND HEAT TRANSFER TUBES IN KRAFT RECOVERY BOILERS

Ameya Pophali[1)], **Markus Bussmann**[2)], **Honghi Tran, and Andrew Jones**[3)]
Pulp & Paper Centre and
Department of Chemical Engineering & Applied Chemistry
[2)]Department of Mechanical and Industrial Engineering
University of Toronto
Toronto, ON, CANADA

[1)]Presently with Clyde Bergemann Inc., Atlanta, GA, USA

[3)]International Paper, Loveland, OH, USA

ABSTRACT

A laboratory study was performed to characterize the supersonic jet-tube interactions that occur in kraft recovery boiler superheater, generating bank, and economizer sections during sootblowing. For the first time, such interactions were visualized using the schlieren technique coupled with high-speed video, and quantified by pitot pressure measurements. Results showed that upon impingement on a tube, a supersonic jet deflects at an angle, forming a weaker secondary jet. Due to a relatively small core length, this jet cannot impinge on an adjacent superheater platen with a significant impact pressure. However, due to the closer tube spacing in the generating bank and economizer, secondary jets impinge on the tubes in the adjacent rows, and may help remove deposits in these regions. Due to its narrow spreading angle, a sootblower jet must be directed close to superheater platens to yield useful jet-deposit interactions. While a jet between superheater platens may propagate unaffected, a jet between generating bank tubes is weakened because of interaction with tubes and increased mixing. A jet between finned economizer tubes decays more quickly than a free jet, but is stronger than the same jet in the generating bank because the fins restrict the spreading of the jet.

INTRODUCTION

The recovery boiler is one of the most important components of a kraft pulp mill. It can also be the main bottleneck in pulp production due to its high susceptibility to deposit buildup on heat transfer tube surfaces. Sootblowers must be operated continuously to control deposit buildup. A substantial amount, 3 to 12%, of the total high pressure steam generated by the boiler is used by the sootblowers that would otherwise contribute to power generation. The steam used also requires more fuels to be burnt in the boiler, which is generally costlier than the lost power generation. As a result, optimizing sootblowing to minimize steam consumption and maximize deposit removal is important.

Depending on the flue gas temperature and heat transfer requirements, tubes in the different sections of a recovery boiler have different spacing between them. Tubes in the superheater region of the boiler are arranged in platens with large side-to-side spacing (e.g. 10”-12”), whereas those in the generating bank and economizer are placed much closer together (e.g. 2.5”) due to the lower flue gas temperature. This smaller spacing is comparable to the sootblower jet size; the sootblower nozzle exit diameter is usually slightly larger than 2.5 cm (1”). Tubes in modern generating banks and economizers are equipped with fins to increase the heat transfer area. These fins may alter the jet impingement flow field. Moreover, a sootblower jet almost always interacts with the first tube of any given row of tubes during sootblowing. This interaction governs the subsequent jet flow.

Conventionally, the performance of a sootblower jet in removing deposits has been correlated with the jet peak impact pressure (PIP) [1], which is the pressure a pitot tube would measure when inserted into the jet at its centerline. Since a sootblower jet is supersonic, it is sensitive to any obstacle or disturbance in its flow. An obstacle in a supersonic flow creates a series of complicated shock and expansion waves, which, in the case of a jet, can directly affect the jet structure, and hence jet strength (PIP) and penetration. If the sootblower jet PIP is reduced due to its interaction with tubes, then the jet may not be able to remove deposits, particularly those away from the

nozzle, leading to deposit bridging and flue gas passage plugging. As such, understanding how a jet interacts with tubes in the different arrangements in a recovery boiler is important.

'Seeing' such jet-tube interaction will provide valuable understanding of the flow field during sootblowing. Several sootblowing studies have been performed at the University of Toronto in the past which involved either investigating the breakup of artificial deposits by a supersonic air jet [2, 3], numerically simulating sootblower jet flow [4, 5], or measuring sootblower jet force in-situ [6, 7]. However, the interaction of a sootblower jet with tubes has never been visualized to date. This is understandable because of the hostile conditions inside the boiler, and because the sootblower jets cannot be seen by the naked eye, or via a regular photographic process.

One way to visualize such flows is in the laboratory by taking advantage of the shock and expansion waves in these jets, which create density gradients, and hence, refractive index gradients in the jet fluid. Such refractive index gradients can be captured by special optical techniques such as Schlieren. Therefore, the main objective of this study was to characterize the supersonic jet-tube interactions that take place in typical recovery boiler superheater, generating bank and economizer sections. The study is divided into two parts: 1) jet interaction with a single tube, and 2) jet interaction with different tube arrangements. A portion of this work on jet-tube interaction with model superheater platens was presented earlier [8]. This paper presents comprehensive results on the interaction with all three tube arrangements.

EXPERIMENTAL DESIGN AND METHODOLOGY

This study involved the following setup: 1) custom-designed jet impingement apparatus consisting of scaled-down models of a typical sootblower nozzle and boiler tubes, 2) high speed schlieren flow visualization system, 3) custom-designed and built pitot probe and positioning system, 4) control and data acquisition system, and 5) image processing software.

Jet Impingement Apparatus

The main components of the apparatus were ¼ scale models of a typical sootblower nozzle and boiler tubes. The nozzle was a convergent-divergent design with a throat diameter d_t = 0.45 cm and an exit diameter d_e = 0.74 cm. Air was used in these experiments for reasons of safety and simplicity. For the lab jet to be dynamically similar to an actual sootblower jet, four characteristics of the lab jet were achieved as close as possible to those of an actual sootblower jet [9]: (1) gas specific heat ratio, γ (= c_p/c_v), (2) nozzle exit Mach number, Ma_e, (3) pressure ratio, PR (ratio of jet static pressure at the nozzle exit to the ambient pressure), or in other words, jet structure (under/overexpanded), and (4) jet spreading rate (which depends on the ratios of the velocities and densities of the jet and the surrounding gas stream [10]).

Figure 1 shows the experimental apparatus. The nozzle was fixed on a two-direction slider arrangement on a workbench. Compressed air from a high pressure supply cylinder was stored in a second buffer cylinder and supplied to the nozzle through a solenoid valve such that the pressure at the nozzle inlet was 2.14 MPa (310 psig), similar to that of an actual sootblower. The nozzle inlet pressure was maintained at this value for all experiments generating a slightly underexpanded jet (PR > 1) with Ma_e = 2.5 for 0.2s. The jet impinged on model tubes placed in front of the nozzle; the resulting interaction was visualized using the schlieren technique and captured by a high-speed camera.

High-Speed Schlieren System

A conventional two-mirror, z-type schlieren system was used for flow visualization. The system consisted of two parabolic Pyrex mirrors (focal length 152 cm or 60" and diameter or field-of-view 14 cm or 5.5"), a continuous halogen light source with adjustable aperture, and a knife edge. The high-speed camera was operated at 6010 frames/s with an exposure time of 150 μs. The images were captured as 504 pixel x 504 pixel greyscale images.

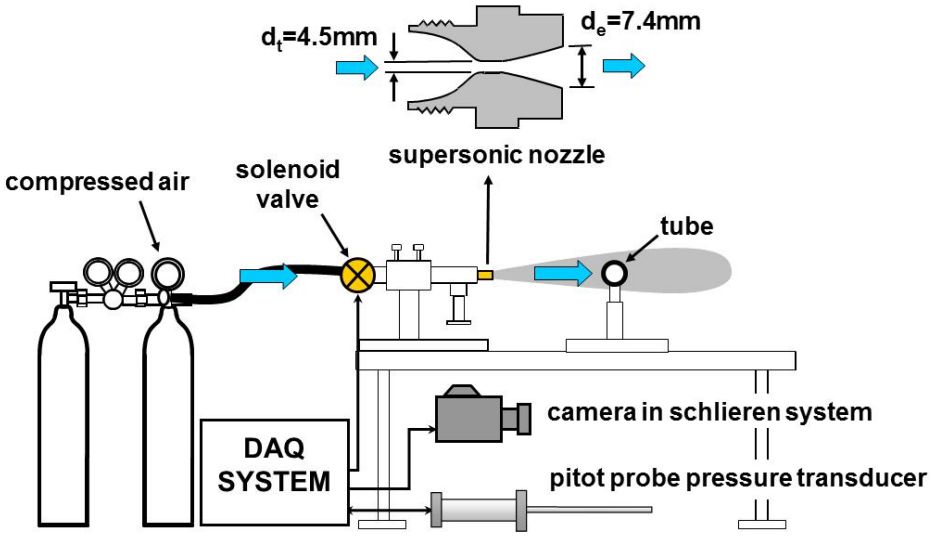

Figure 1. *Experimental apparatus.*

Pitot Probe and Positioning System

A special pitot probe was designed and fabricated to measure the pitot pressure of the supersonic jet. The probe interior was designed so that the jet would completely pressurize the probe within 0.2s, and yield a stable, reliable, and accurate reading, while the tip was a square-cut orifice to make the probe insensitive to minor pitch and yaw misalignments [11]. The other end of the probe was connected to a pressure transducer.

The repeatability of measurements was confirmed by examining the variability of jet supply pressure and free jet centreline pitot pressure. Based on 25 measurements, the average supply pressure was found to be 2.14 MPa (310 psig) with a standard deviation of only 14 kPa (2 psi) or 0.7% of the supply pressure. The maximum standard deviation in the transducer signal obtained at different locations along the free jet axis was determined from at least 3 measurements to be 70 kPa (10 psi) for a pitot pressure equal to 0.84 MPa (122 psig), that is, 8.3% of the pitot pressure. In this paper, error bars for each data point shown in a graph are equal to +/- 1 standard error. Accuracy of the pitot probe was confirmed by comparing the pitot pressure measured at the nozzle exit to that calculated theoretically (p_{o2}) using the normal shock relation (eq. (1)), Ma_e, and the supply pressure (p_{o1}), for four different supply pressures. The error relative to the calculated pressure was only 1% at a supply pressure of 2.15 MPa (312 psig).

$$\frac{p_{o2}}{p_{o1}} = \left(\frac{(\gamma+1)Ma_e^{\,2}}{2+(\gamma-1)Ma_e^{\,2}} \right)^{\frac{\gamma}{\gamma-1}} \left(\frac{\gamma+1}{2\gamma Ma_e^{\,2}-(\gamma-1)} \right)^{\frac{1}{\gamma-1}} \quad \ldots (1)$$

Control and Data Acquisition System

A control and data acquisition system, consisting of National Instruments hardware and Labview software, was setup to control the solenoid valve, high-speed camera, and pitot probe pressure transducer, and to acquire data from the transducer. The images and transducer signal were subsequently processed and analyzed.

Image Processing

Wherever appropriate, schlieren images of the steady-state flow field captured by the high-speed camera were first averaged using image processing software, ImageJ [12], then contrast-enhanced, and then used to measure flow characteristics such as jet angles.

INTERACTION BETWEEN A JET AND A SINGLE TUBE

Experimental Parameters

Four main parameters govern the interaction between a supersonic jet and a tube - (1) the jet structure (under/overexpanded), as characterized by PR, (2) the nozzle-tube distance (x), (3) the jet diameter (d_e) relative to the tube diameter (D), and (4) the offset (or eccentricity) between the jet and tube centrelines (ε). In this work, the same jet was used in all experiments, maintaining PR constant. As a result, experiments were performed to investigate the effects of the other three parameters on jet-tube interaction. However, since varying the offset influenced the interaction between the jet and tube strongly, only these results are presented here. Only the offset between a sootblower jet and a row of tubes changes continuously inside a boiler because of sootblower translation; the other parameters are more or less fixed for a given installation.

The nozzle-tube distance was fixed at 5 cm ($6.8d_e$), which at ¼ scale corresponds to the typical distance inside a boiler. The offset was increased incrementally from 0 to a value at which the jet was so far from the tube that no interaction occurred. The interaction was visualized at each offset. Tubes of three outer diameters were used – small (1.27 cm or 1/2”), medium (1.91 cm or 3/4”), and large (2.54 cm or 1”). The small tube (1/2”) was a ¼ scale typical superheater tube.

Results

Effect of offset. Figure 2 (on page 4) shows schlieren images of jet-tube interaction for the small and medium tubes. The offset is normalized by the tube outer radius R. Similar results were obtained for the large tube, and so are not presented here. Figure 2 shows that upon impingement on a tube at an offset, the supersonic jet deflects at an angle that depends on the offset. At zero offset (image a in Figure 2a), when the jet impinges on the tube head-on, the jet splits into two, small symmetric jets (the lower jet cannot be seen because of the tube stand). As the offset increases (image b onwards), the interaction between the jet and the tube weakens, and the upper jet deflects less and becomes stronger, whereas the lower jet becomes weaker. Beyond a certain offset (image i), there is no interaction between the jet and the tube, and no jet deflection occurs.

Figure 3 below schematically shows the interaction between a supersonic jet and a cylinder. The impinging jet is termed the ‘primary’ jet and the deflected jet the ‘secondary’ jet; these terms are used to refer to these jets in this paper. When the primary jet impinges on a tube, a shock wave forms upstream of the tube. The flow accelerates from this impingement region, separates from the tube surface, and forms a secondary jet some distance downstream. The schlieren images show the presence of compression and expansion waves in the secondary jets, indicating that they are supersonic.

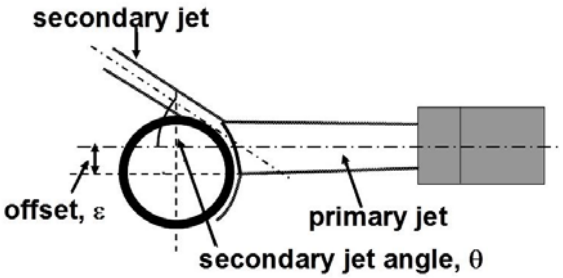

Figure 3. *Formation of secondary jets.*

Comparing the interaction at 0 offset for the two tubes in Figure 2 (images a in Figures 2a and 2b) shows that secondary jets form in the case of the small cylinder, but not in the case of the medium cylinder. For the medium cylinder, a single secondary jet only appears at a non-zero offset (0.25R). Images of the interaction with the large cylinder showed similar phenomena, and the offset at which a secondary jet formed was found to be even greater (0.59R). Thus, for cylinders much larger than the jet, secondary jets do not form at small offsets; the offset at which a secondary jet first appears increases with the cylinder size.

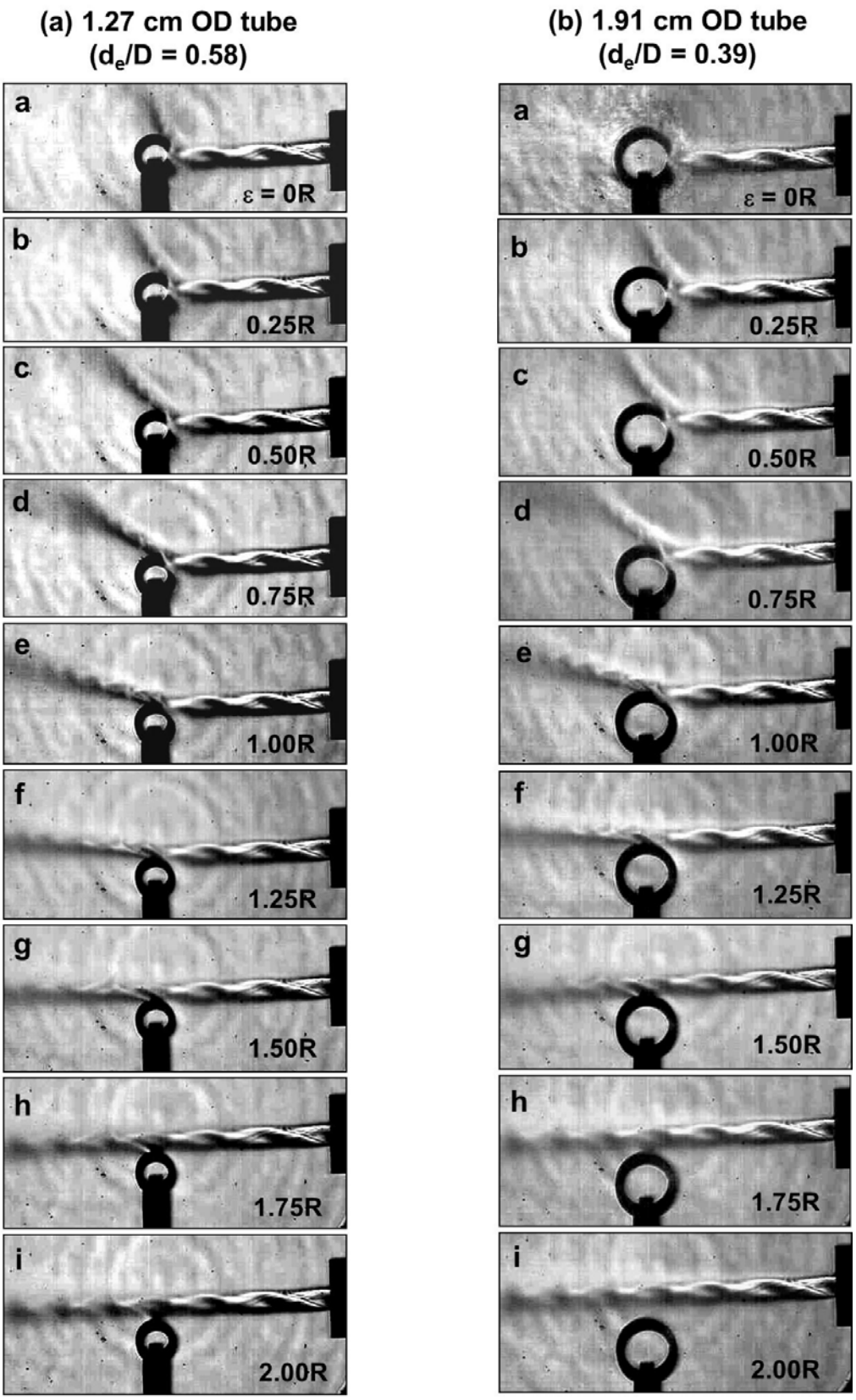

Figure 2. *Jet impinging on small and medium tubes at different offsets ($x = 6.8d_e$).*

INTERACTION BETWEEN A JET AND TUBE ARRANGEMENTS

Interaction with Model Superheater Platens

Model superheater platens. Two ¼ scale model superheater platens were constructed and mounted on supporting stands, as shown in Figure 4. Each platen consisted of five 1.27 cm (1/2") OD steel tubes welded together in a straight line. The stands were adjustable so that the platen could be positioned at different offsets relative to the nozzle.

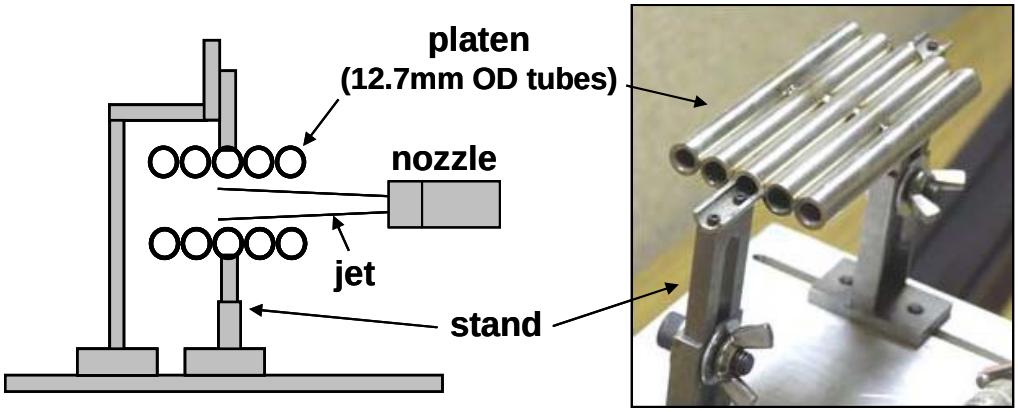

Figure 4. *Model superheater platens.*

Effect of offset. Schlieren images of a jet impinging on a platen at different offsets are presented in Figure 5. Secondary jets form when the primary jet impinges on the first tube of the platen, up to an offset of 0.95R (images a-d). Beyond that, only the primary jet remains, and interacts with all of the tubes of the platen, forming a complicated sequence of shock and expansion waves (images e-g). The interaction in image g is the weakest; for larger offsets, the jet ceases to interact with the tubes (images h and i). This is because of the very low spreading rate of a supersonic jet; the jet diffuses very little in the core region.

Jet midway between platens. Figure 6 shows the flow of a jet exactly between two platens and reinforces the point made in the above discussion, that there is no interaction between the jet and the platens, or deposits on the platens when sootblowing between platens (unless the deposits are so big that they block the flue gas passage); the jet propagates undisturbed between them. Noticeable interaction takes place only when the jet actually 'touches' a platen. This can also be shown by comparing the typical spacing between superheater platens to the radial spread of a jet. Figure 7 shows the measured jet radius as a function of axial distance from the nozzle. Half of the typical inter-platen spacing is also shown. The figure shows that there will be no interaction between the jet and the platens.

Interaction with a Model Generating Bank

Model generating bank. A ¼ scale model of a generating bank was designed and built, consisting of 40 aluminium tubes of outer diameter 1.43 cm (9/16") (Figure 8). The tubes were arranged in a 4x10 inline array, in which the 10 tubes were positioned in the direction of jet propagation. The inter-tube spacing (surface-to-surface) was 1.27 cm (1/2") in each direction of the array. To allow optical access for the schlieren system, the tubes were rigidly fixed between two specially designed and fabricated quartz plates mounted to steel frames. The distance between the nozzle and the surface of the first tube of the bank was set at 5 cm. The nozzle was fixed on an adjustable stand, to yield different offsets between the nozzle and the tube.

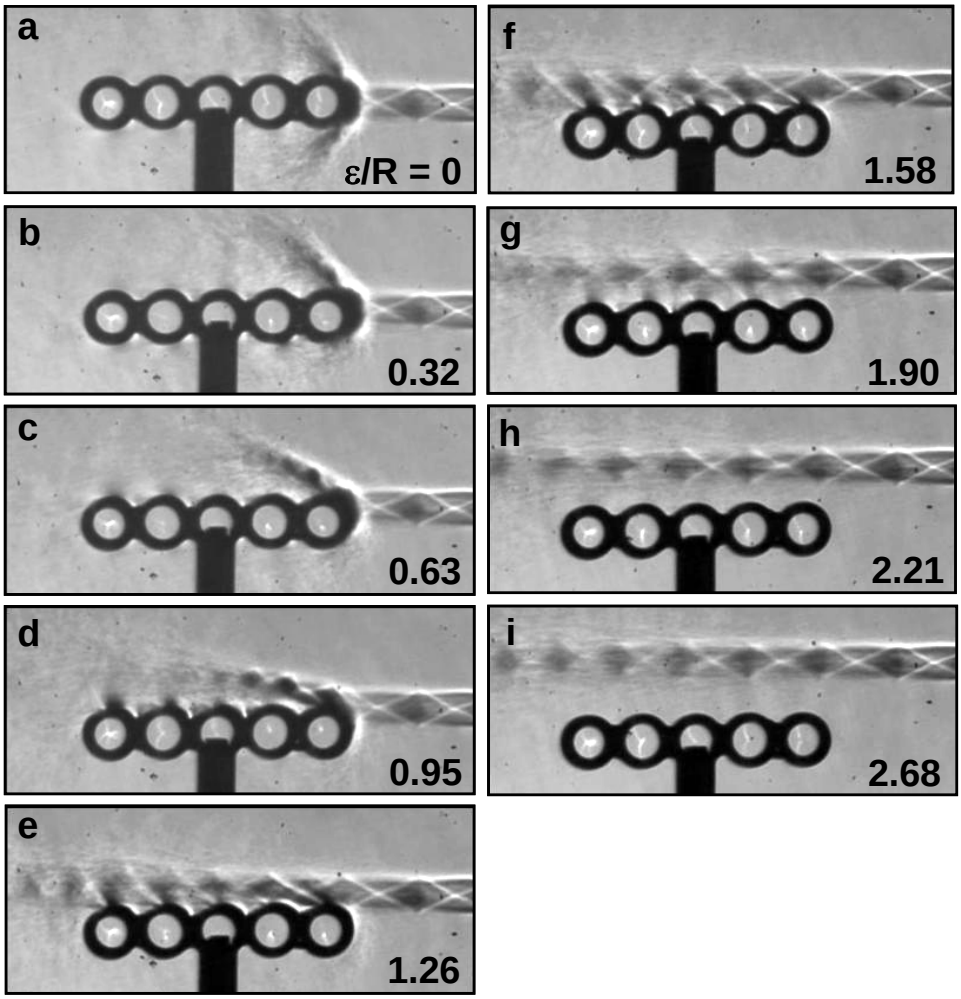

Figure 5. *Jet impingement on a platen at different offsets.*

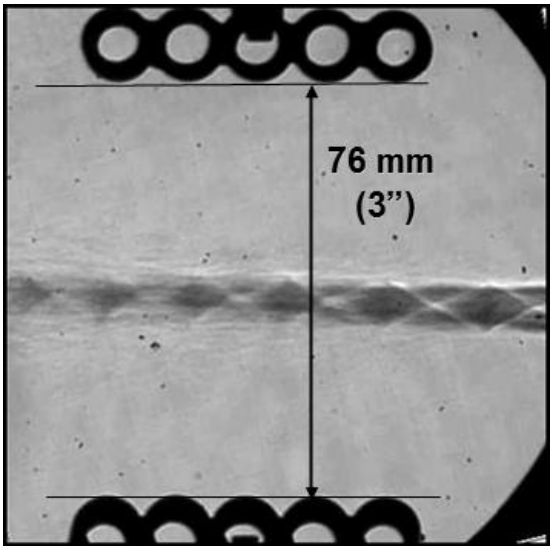

Figure 6. *Jet midway between two platens – no interaction.*

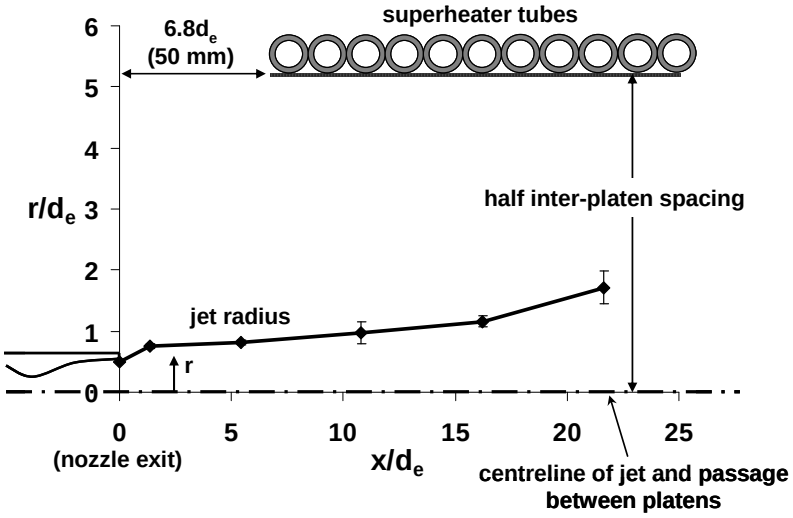

Figure 7. *Radial spread of a jet imposed on a typical superheater platen arrangement.*

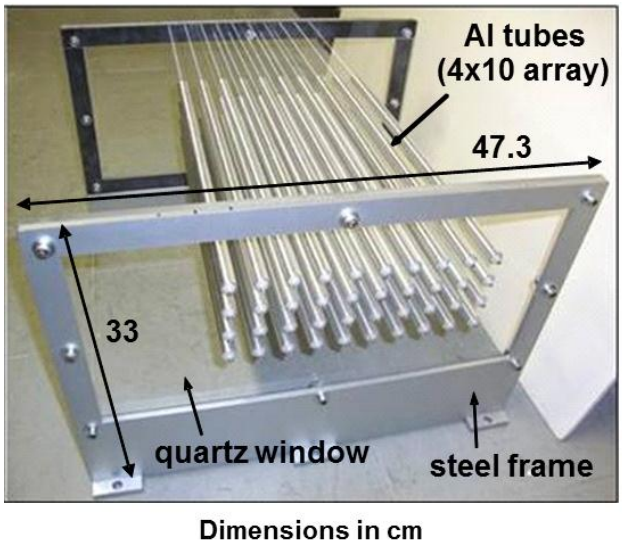

Figure 8. *Model generating bank.*

Effect of offset. Figure 9 shows images of the jet impinging on a model generating bank tube at different offsets. At zero offset, the jet impinges directly on the first tube of the tube bank (head-on impingement), whereas at maximum offset ($\varepsilon/R = 1.9$ or $\varepsilon = 1.35$ cm), the jet propagates midway between two tubes. Images f-h show that at large offsets, only the primary jet exists and interacts with the tubes; secondary jets form only at small offsets (images a-e), as expected. An interesting and important phenomenon can be observed now: because the tubes are close to each other, the secondary jets that form during impingement of the primary jet, in turn impinge on the neighbouring tubes in the adjacent rows. The impinged tube depends on the offset. In image a, two secondary jets impinge on the sides of the first tubes in the adjacent rows. In images b and c, a single stronger secondary jet flows between the first two tubes of the adjacent row. In images d and e, a still stronger secondary jet impinges on the second and third tubes in the adjacent row respectively. In these images, even the supersonic portion of the secondary jet, that is, its core region, impinges on the adjacent tubes.

Examination of the flow field further downstream in the tube bank showed that there is no jet flow in this region when the offset is small, because the jet is fully consumed upstream in the form of a secondary jet. Only when the

offset is large (1.3R onwards in Figure 9) can the jet flow between two rows of tubes (without forming secondary jets), and thus penetrate further into the tube bank. Maximum penetration of a jet occurs when the jet is exactly midway between the tubes. However, image h of Figure 9 shows that even in this position, there is some interaction between the jet and the tubes, which may affect jet strength. Consequently, this particular flow scenario was studied in detail.

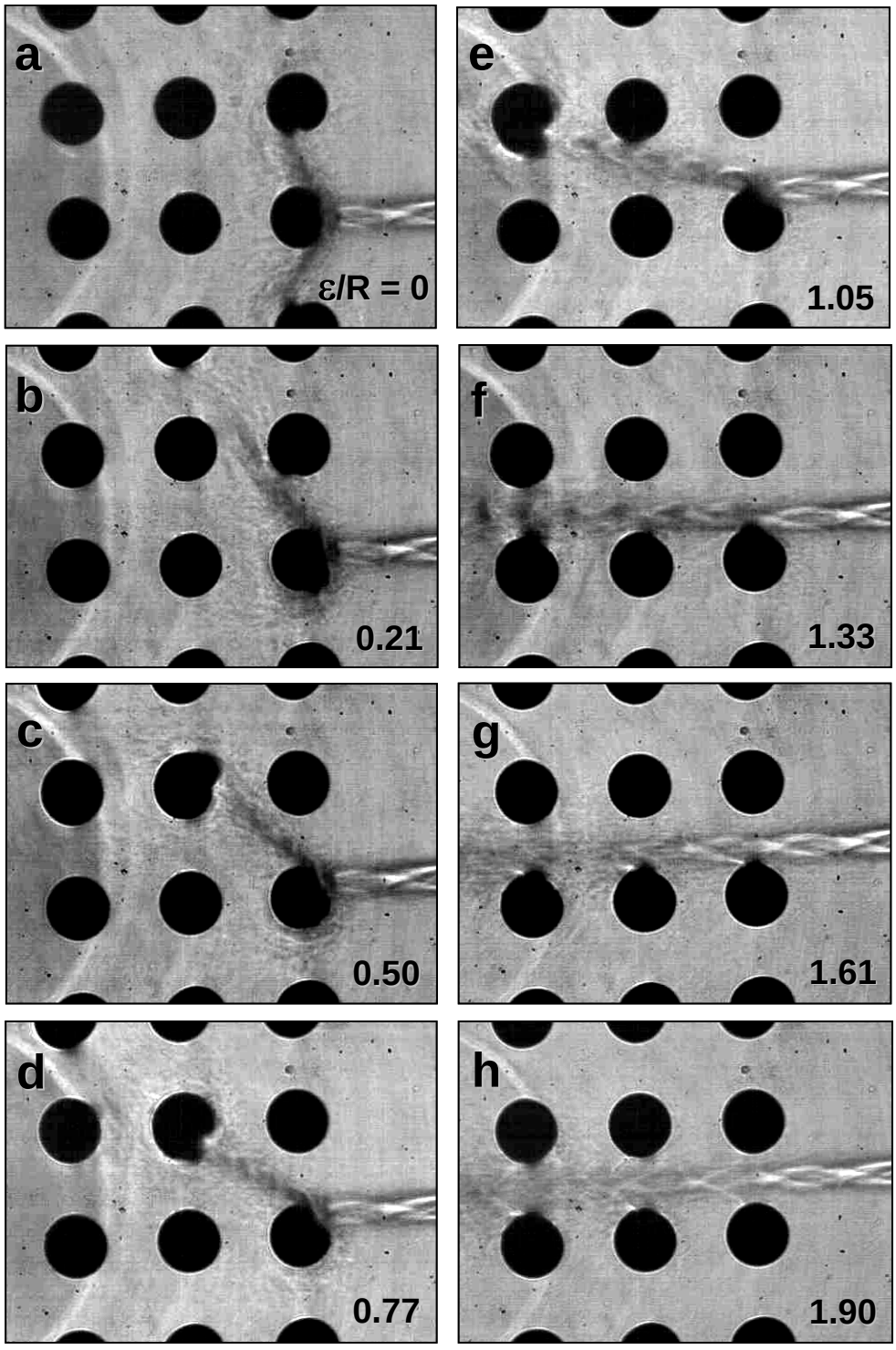

Figure 9. *Jet flow into a model generating bank, at different offsets.*

Jet midway between two rows of tubes. For this scenario, the nozzle was fixed such that the jet was midway between two rows of tubes. The pitot probe was used to measure the impact pressure at the jet centreline and along the edge of one of the tube rows. Figure 10 shows these impact pressure profiles. The centreline impact pressure profile of a free jet is shown for comparison, along with the approximate position of the tubes.

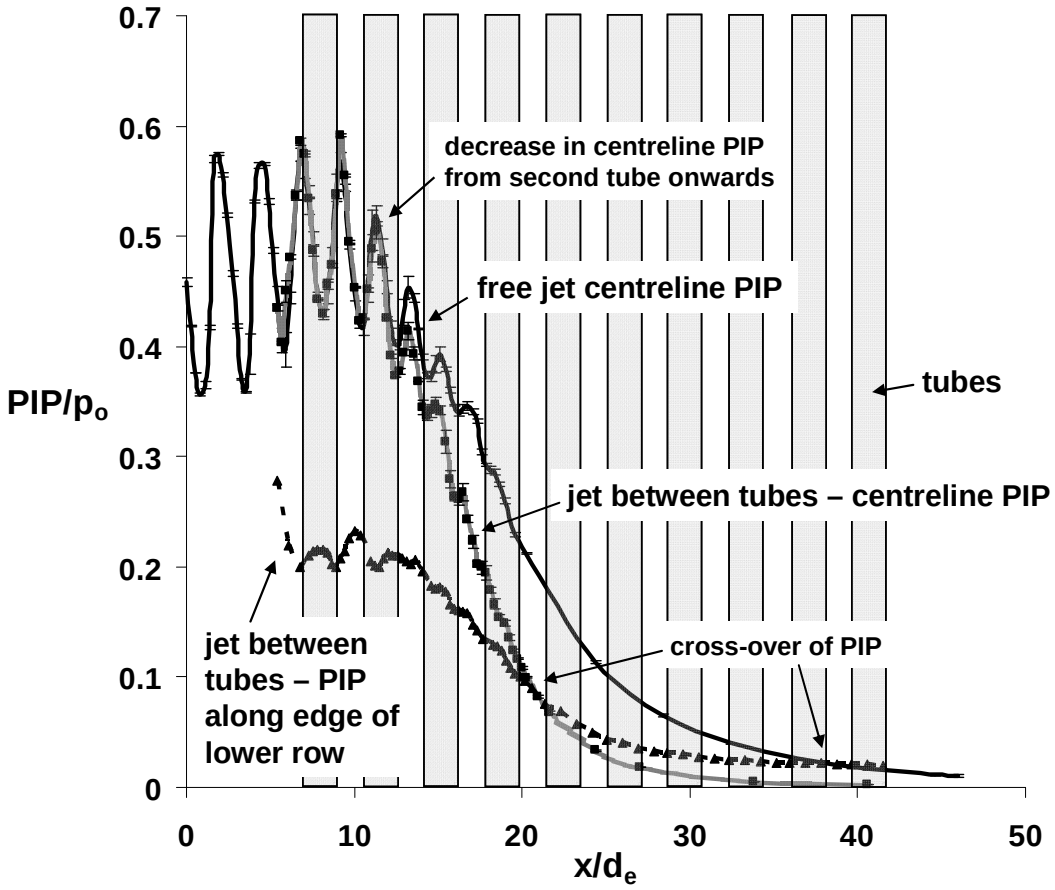

Figure 10. *Peak impact pressure profiles of a jet midway between model generating bank tubes.*

The centreline impact pressure of the jet between the tubes remains the same as that of the free jet until the second tube ($x/d_e = 12.4$); beyond the second tube, PIP decreases relative to that of the free jet. The decrease is seen in both the supersonic and subsonic portions of the jet; in the supersonic portion, the shock cells are weaker than those in the free jet, and in the subsonic portion, the rate of decrease of the impact pressure is higher than that in the free jet. This decrease can be attributed to a number of causes:

1. The interaction of the jet boundary or shear layer with the tube surfaces leads to the formation of boundary layers on the surfaces, in which the kinetic energy of the flow is dissipated as heat through the viscous motion of the fluid layers. The dissipation of energy leads to a decrease in the jet axial momentum, which manifests itself as a decrease in PIP.
2. At steady-state, expansion waves form on the first two tubes of a row of generating bank tubes. As jet air passes through the expansion waves on the first tube a small amount of that air deviates outwards from the axial flow direction and impinges on the second tube. This weaker flow remains attached to that tube via the Coanda effect and is re-entrained into the jet, increasing jet mixing. This process repeats itself and intensifies further downstream. Since the second tube lies in the supersonic portion of the jet, the decrease in PIP observed in Figure 10 starts in the supersonic portion of the jet, and weakens the shock cells (see [9] for a detailed explanation).
3. Finally, the jet spreads laterally due to confinement by the tubes, and its momentum is redistributed over a greater cross-sectional area.

As was done for the superheater platens, Figure 11 illustrates the radial spread of a jet superimposed on a schematic of the typical spacing between generating bank tubes. The figure clearly shows that for a jet directed midway between tube rows, the jet boundary just touches the first tube of the row, and is interrupted by the second tube. As a result, jet-tube interaction begins from the first tube and becomes stronger from the second tube onwards, corroborating the result obtained from Figure 10.

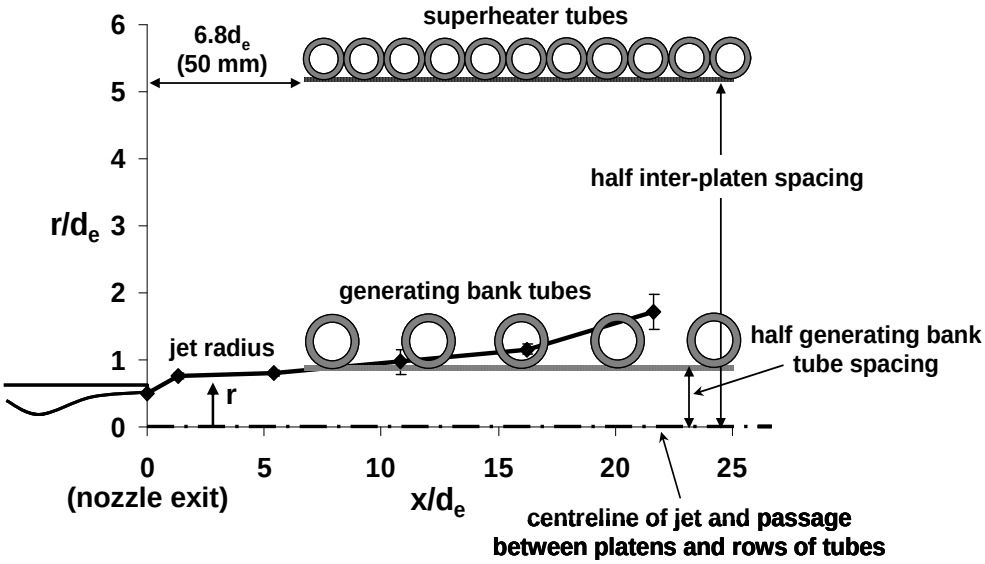

Figure 11. *Radial spread of a jet imposed on a typical generating bank tube arrangement.*

Figure 10 also shows that the impact pressure along the edge of a row is lower than that along the centreline. Along the edge of a row, the probe averages the PIP mainly across the shear layer of the jet and over some internal portion; thus the velocity of the jet in these regions is lower than that closer to the centreline.

Another interesting phenomenon observed in Figure 10 is that beyond the jet core (approximately 18 nozzle diameters), in the region where the jet turns subsonic from supersonic, the PIP along the edge of the row of tubes exceeds the centreline PIP, and its rate of decrease is also slower. At a larger distance, the PIP along the edge also crosses over the centreline PIP of a free jet. The tubes restrict the entrainment and spreading of the jet, because of which the jet spreads laterally, redistributing its momentum. A free jet spreads unrestricted with distance, thus the centreline PIP of a free jet decreases continuously.

Interaction with Model Economizer Tubes (Finned Tubes)

Model economizer section. Due to lack of data on economizer tube dimensions in the open literature, a survey of typical economizer tube arrangements in recovery boilers was conducted with three major boiler manufacturers as participants. Results of the survey can be found in [9], and were used to design two identical ¼ scale rows of economizer tubes with fins. Figure 12a schematically shows one of these rows. It consisted of six 1.1 cm (7/16") OD tubes with fins welded on both the windward and leeward sides, with zero front-to-back spacing. Fins on the outer sides of the end tubes had a width equal to the tube outer diameter, and fins between two tubes had twice that width. The model was supported on the same stands used for the model superheater platens, which allowed the offset between them and the nozzle, as well as the spacing between the two rows, to be varied. Figure 12b shows the assembly. Based on the survey results, the spacing between the two rows was fixed at 1.27 cm (1/2"), corresponding to 2" spacing in a boiler.

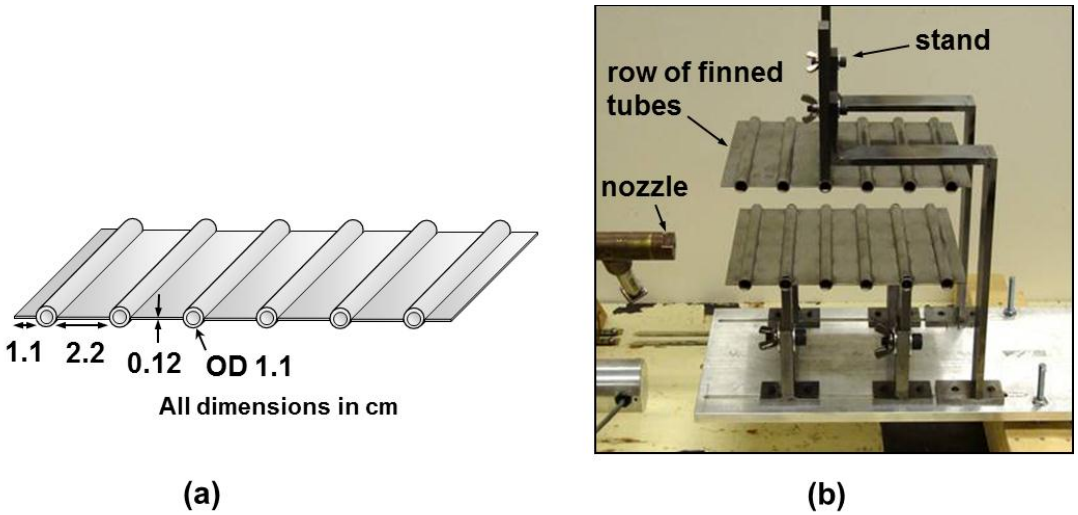

Figure 12. *Model economizer tubes: (a) schematic of a row; (b) tube assembly.*

Effect of offset. Figure 13 shows images of a jet impinging on a row of finned tubes at different offsets. As expected, secondary jets form when the jet impinges on the first tube of a row. However, in this case the secondary jets that form at 0 offset are strongly affected by the leading fin. Image a in the figure shows that upon impingement on the fin, the primary jet splits into two parts (one above the fin and one below) which deviate slightly from the original axial flow direction (from right to left in the image). Thereafter, they impinge on the first tube, further deflecting from their original flow direction. Due to multiple interactions with the tip of the fin, the fin surface and the tube, these secondary jets are weaker than those observed in the superheater and generating bank. Except for the effect of the fin, the behavior of these secondary jets was found to be similar to that presented earlier.

Jet midway between two rows of tubes. Figure 14 presents the PIP profiles of a jet positioned midway between two rows of economizer tubes. The centreline PIP in the supersonic portion (or core) of a jet midway between the economizer tubes is unaffected by the presence of the tubes. However, the PIP decreases compared to the free jet in the subsonic portion of the jet (beyond 18 nozzle diameters). This is due to the increased level of mixing in the jet, particularly just upstream and downstream of the tubes (which are regions of recirculation and wake respectively), and because the jet spreads in the lateral direction. The finned tubes form walls confining the jet between them, and restrict the spreading of the jet in the direction normal to the walls. As a result, the jet spreads laterally to adjust to the almost planar confinement, its momentum redistributes over a greater cross-sectional area, and from about the third tube onwards where the jet turns subsonic, the jet PIP decreases.

Although the economizer and generating bank tubes are equally spaced (1.27 cm or 1/2” in the present experiments), the jet centreline PIP between the economizer tubes remains stronger for a greater distance than between the generating bank tubes because of the restricted entrainment and spreading of the jet. In the generating bank, the open gaps between the tubes allow some small portion of the jet air to flow around the tubes, and entrain air from the surrounding rows. The fins in the economizer, on the other hand, prevent such entrainment.

The PIP along the edge of a row of tubes is much lower than the centreline PIP, because at the edge, the pitot probe measures the PIP in the outermost part of the jet. PIP increases with distance up to about 18 nozzle diameters because of the spreading of the jet, and then decreases continuously with distance due to mixing.

As was observed in the PIP profiles of a jet in a generating bank (Figure 10), the PIP along the edge of a row of tubes in the economizer also eventually exceeds the PIP along the jet centreline. The increase in PIP is greater for the economizer than the generating bank, because the entrainment and spreading is restricted much more by the fins in the economizer.

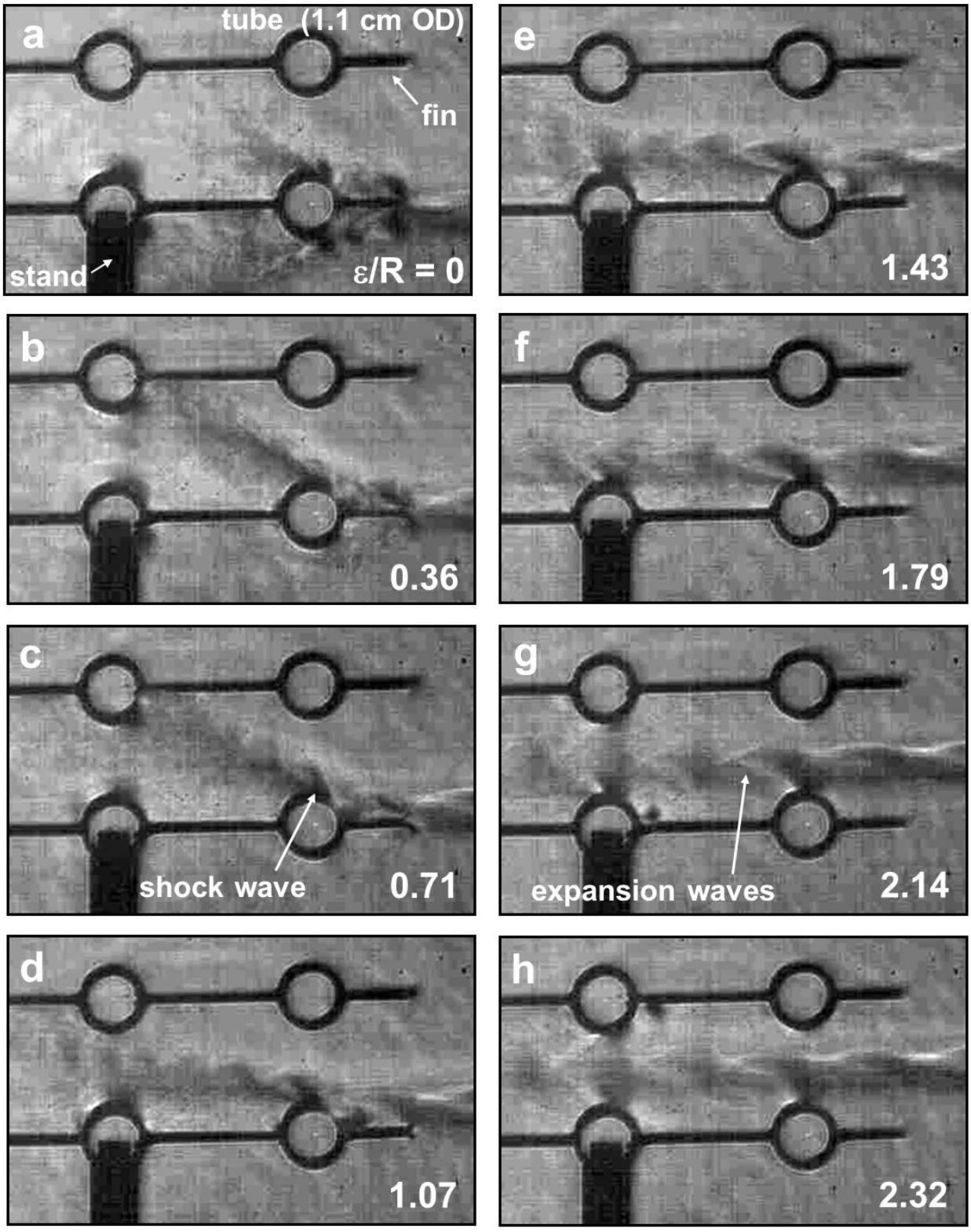

Figure 13. *Jet impinging on economizer tubes at different offsets.*

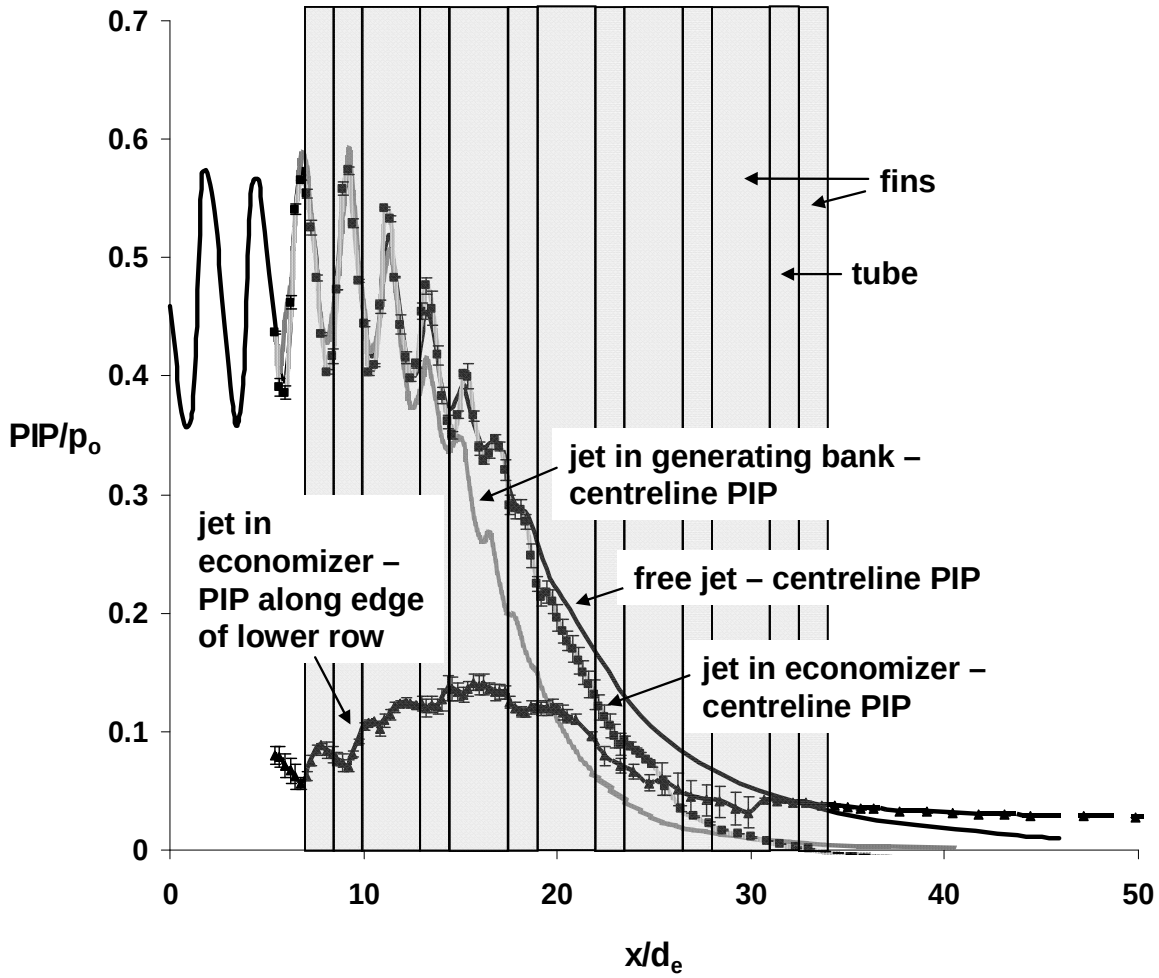

Figure 14. *Peak impact pressure profiles of a jet midway between model economizer tubes.*

PRACTICAL IMPLICATIONS

1. For all three tube arrangements (superheater, generating bank, and economizer), secondary jets form when a primary jet impinges on the first tube of a row of tubes. So long as secondary jets form, there will be little or no jet flow beyond the first few tubes of these arrangements (third or fourth tube in the superheater and generating bank sections, and the second tube in the economizer section). Hence, any deposits beyond the first few tubes do not experience the sootblower jet for a significant amount of time. Secondary jets become practically more important at closer tube spacing. Due to a large inter-platen spacing, a secondary jet cannot effectively remove a deposit on an adjacent superheater platen. However, it impinges on the closely-spaced tubes in a generating bank and economizer, and may exert a significant impact pressure on deposits clinging to those tubes, possibly removing some. Even if the deposits are too hard to break, the secondary jets may help erode them.

2. To shed more light on the above finding, secondary jet PIP was measured along the jet centerline in another study. The measurements showed that secondary jets retain a strong PIP for appreciable distances downstream of the tube only at large offsets, and not as far as a primary jet. Secondary jet PIP data shows that the PIP exerted by these jets on the adjacent tubes in the model generating bank is slightly less than half the average PIP in the primary jet core. As a result, these jets will not exert a very high PIP on the deposits attached to generating bank and economizer tubes, but they may help erode such deposits, which are inaccessible directly from the sootblower nozzle. Deposits in the generating bank are a mixture of carryover and fume deposits, and in some locations may be hard and brittle; those in the economizer are primarily fume, and are thin and powdery. Secondary jets may help remove such deposits.

3. Another consequence of secondary jet impingement is that it may contribute to tube erosion. In the past, North American recovery boiler operators have consistently reported thinning of generating bank tubes, very near the mud-drum of the bank, and occasionally at sootblower elevations [13]. The most severe metal loss is found on the tubes closest to the sootblower lanes, and the severity decreases in tube rows further away. The thinning is very localized, and only small areas around the tube circumference are affected. Studies conducted by the Pulp and Paper Research Institute of Canada (PAPRICAN) [13] showed this thinning to be most likely caused by a repeated cycle of under-deposit corrosion followed by removal of accumulated corrosion product by sootblowers. Although the present experiments were conducted for a different objective, their findings appear consistent with this experience. As Figure 9 shows, secondary jets impinge only on generating bank tubes closest to the sootblower, and at an angle that corresponds to the thinning locations indicated in [13]. The results suggest that the secondary jets may be the means by which the sootblower steam reaches the tubes behind the first tube of any given row.

4. Due to the very low spreading rate of a supersonic jet, deposits clinging to the side of a platen will not be exposed to a sootblower jet that is offset by even a small distance from the deposits. Furthermore, much of the steam that the sootblower blows between platens is wasted, as only small offsets yield useful jet-deposit interaction. The situation is better in the generating bank and economizer sections, because the tube spacing is small and the jet interacts with the deposits more frequently. However, the close spacing affects sootblower jet strength (PIP) and penetration between tubes. While a jet flows unaffected between superheater platens, the centreline PIP of a jet between generating bank tubes decreases relative to that of a free jet from the second tube onwards. As a result, deposits deeper in the generating bank may be hard to clean. For the same spacing between rows of tubes, the centreline PIP of a jet between finned economizer tubes also decreases, but at a greater distance from the nozzle than in a generating bank. Essentially, a jet is stronger and penetrates deeper in a tube arrangement consisting of finned tubes, than in an arrangement of just finless tubes, as the fins restrict the entrainment and spreading of the jet.

The above implications are briefly summarized in Table I.

Table I. *Summary of sootblower jet-tube interaction in the superheater, generating bank, and economizer.*

	Superheater	**Generating Bank***	**Economizer***
Primary jet	• Only effective at small offsets to a platen. • Ineffective when directed midway between platens.	• Strong interaction with tubes. • When directed midway between tube rows, axial PIP decreases to less than 50% of its average value in the core by the fourth tube, and to less than 10% by the sixth tube.	• Strong interaction with tubes. • When directed midway between tube rows, axial PIP decreases to less than 50% of its average value in the core just downstream of the third tube, and to less than 10% by the fifth tube (note that there are fins between the tubes). • Jet remains stronger than in a generating bank.
Secondary jet	Insignificant impact on deposits on adjacent platens.	May help erode deposits on the second and third tubes inside the bank.	May be sufficiently strong to remove soft, fluffy deposits on the second and third tubes inside the economizer.

*The PIP values and tube locations presented are specifically for the model geometries considered in this study.

CONCLUSIONS

Part 1 of this study showed that upon impingement on a tube, a sootblower jet deflects at an angle, forming a weaker secondary jet. The angle and strength of the secondary jet depend on the offset between the jet and tube centerlines. Once the primary jet is only a small distance away from the tube, interaction between the jet and tube ceases due to the very low spreading rate of the jet.

Part 2 showed that a sootblower jet must be directed close to superheater platens to yield useful jet-deposit interactions. Continuous sootblowing between platens is justified only if large deposits significantly block the space between the platens. While a jet flows unaffected between platens, a jet between generating bank tubes becomes weaker than a free jet, because of interaction with tubes and increased mixing. The centreline peak impact pressure begins to decrease in the jet core. Consequently, deposits beyond the first few tubes of a row experience a weaker sootblower jet. A jet between finned economizer tubes also decays more quickly than a free jet, but is stronger than the same jet in the generating bank. The strength (centreline peak impact pressure) and hence the deposit removal capability of the jet diminish only slightly beyond the supersonic portion of the jet. This is because the fins restrict the entrainment and spreading of the jet.

Secondary jets become more effective at closer side-to-side tube spacing. Due to a small core length and large inter-platen spacing, a secondary jet cannot impinge on an adjacent superheater platen with a significant peak impact pressure, and so has little chance of effectively removing a deposit there. However, due to the closer side-to-side tube spacing in the generating bank and economizer, secondary jets impinge on the tubes in the adjacent rows, and may help remove deposits on them.

ACKNOWLEDGEMENT

This work was conducted as a part of the research program on “Increasing Energy and Chemical Recovery Efficiency in the Kraft Process,” jointly supported by the Natural Sciences and Engineering Research Council of Canada (NSERC) and a consortium of the following companies: Andritz, Babcock & Wilcox, Boise Paper, Carter Holt Harvey, Celulose Nipo-Brasileira, Clyde-Bergemann, DMI Peace River Pulp, Fibria, International Paper, Irving Pulp & Paper, Metso Power, MeadWestvaco, StoraEnso Research, and Tembec. Their financial support is greatly appreciated.

REFERENCES

1. Jameel, M.I., Cormack, D.E., Tran, H.N., and Moskal, T.E., “Sootblower Optimization Part I: Fundamental Hydrodynamics of a Sootblower Nozzle and Jet”, TAPPI Journal, Vol. 77, No. 5, pp. 135-142 (1994).

2. Kaliazine, A., Piroozmand, F., Cormack, D.E., and Tran, H.N., “Sootblower Optimization Part II: Deposit and Sootblower Interaction”, TAPPI Journal, Vol. 80, No. 11, pp. 201-207 (1997).

3. Pophali, A., Eslamian, M., Kaliazine, A., Bussmann, M., and Tran, H. N., “Breakup Mechanisms of Brittle Deposits in Kraft Recovery Boilers - A Fundamental Study”, TAPPI Journal, Vol. 8, No. 9, pp. 4-9 (2009).

4. Tandra, D. S., Kaliazine, A., Cormack, D. E., and Tran, H. N., “Interaction between Sootblower Jet and Superheater Platens in Recovery Boilers”, Pulp & Paper Canada, Vol. 108, No. 5, pp. 43-46 (2007).

5. Emami, B., Bussmann, M., Tran, H. N., and Tandra, D., “Advanced CFD Simulations of Sootblower Jets”, International Chemical Recovery Conference, TAPPI/PAPTAC, Williamsburg VA, Mar. 29-Apr.1 (2010).

6. Saviharju, K., Kaliazine, A., Tran, H. N., and Habib, T., “In-Situ Measurements of Sootblower Jet Strengths”, TAPPI Journal, Vol. 10, No. 2, pp. 27-32 (2011).

7. Tran, H. N., Pophali, A., Bussmann, M., and Miikkulainen, P., “Measurements of Sootblower Jet Strength in Kraft Recovery Boilers – Part II: Results of the 3rd and 4th Field Trials”, TAPPI Journal, *accepted for publication* (2012).

8. Pophali, A., Bussmann, M., and Tran, H. N., “Visualizing the Interactions between a Sootblower Jet and a Superheater Platen”, International Chemical Recovery Conference, TAPPI/PAPTAC, Williamsburg VA, Mar. 29-Apr.1 (2010).

9. Pophali, A., “Interaction between a Supersonic Jet and Tubes in Kraft Recovery Boilers”, PhD thesis, Dept. of Chemical Engineering and Applied Chemistry, University of Toronto, Canada (2011).

10. Papamoschou, D. and Roshko, A., “The compressible turbulent shear layer: an experimental study”, Journal of Fluid Mechanics, 197, pp. 453-477, 1988.

11. Bryer, D. W. and Pankhurst, R. C., *Pressure-probe Methods for Determining Wind Speed and Flow Direction*, H. M. S. O., London (1971).

12. Schneider, C. A., Rasband, W. S., and Eliceiri, K. W., “NIH Image to ImageJ: 25 Years of Image Analysis”, Nature Methods, Vol. 9, p. 671 (2012).

13. Singbeil, D., “Corrosion of Generating Bank Tubes in Kraft Recovery Boilers”, Pulp & Paper Canada, Vol. 95, No. 12, pp. 132-135 (1994).